

DEVELOPMENT OF SPACE INFLATABLE/RIGIDIZABLE STR ALUMINUM LAMINATE BOOMS

Michael Lou and Houfei Fang
Jet Propulsion Laboratory
California Institute of Technology
Pasadena, California

Lih-Min Hsia
Department of Mechanical Engineering
California State University at Los Angeles
Los Angeles, California

ABSTRACT

Development of inflatable structures for space applications has progressed rapidly in the past few years. Noticeable advances have been achieved in several key technology areas, such as system concepts, analysis tools, material selection and characterization, and inflation deployment control. However, many challenges remain to be overcome before the inflatable structures can be actually incorporated into space flight systems. One of these challenges is the development of suitable in-space rigidization methods and many researchers in the space inflatables community are currently working toward this goal. This paper describes the concept and development of a new type of space inflatable/rigidizable structures, called the spring-tape-reinforced aluminum laminate booms (simply, STR booms). Analysis and test results related to buckling capability, effects of stowage, modal characteristics, and dynamic responses of STR booms are presented and discussed. Additional research efforts are also recommended for improving structural integrity of the STR booms, as well as developing load-carrying booms over 50 meters.

INTRODUCTION

Space inflatable structures technology is one of the emerging technologies that can potentially revolutionize the design of large space structural systems. There is a great interest in near-term space applications of inflatable structures and a possibility of enabling several breakthrough missions in the more distant future. In fact, many future NASA missions must use space inflatable structures in order to meet their launch volume and mass goals. This is especially true for missions that will employ flight hardware components and systems of relatively large in-orbit configurations. These include radar antennas, solar arrays, sunshades, solar concentrators, and telescope reflectors. At present, these hardware components and systems commonly use mechanically deployed structures to meet their launch volume constraints. Compared to mechanically deployed structures, space inflatable structures have many distinct advantages, such as much lighter weight, higher packaging efficiency, lower life-cycle costs, simpler design with fewer parts, and higher deployment reliability. In 1997 NASA embarked on a technology development program to advance the inflatable technology and make it available to 21st century space missions. Since that time, much important technological advancement in space inflatable structures, particularly in the areas of controlled deployment, material characterization, and analysis and simulation tools have been achieved. However, space rigidization of inflatable structures remains to be a major technical challenge and must be adequately addressed before space inflatables can be actually applied to future missions.

Copyright © 2000 by the American Institute of Aeronautics and Astronautics, Inc. The U.S. Government has a royalty-free license to exercise all rights under the copyright claimed herein for governmental purpose. All other rights are reserved by the copyright owner.

For space applications, the desired features for space rigidization include: (1) being lightweight and easily adaptive to high-efficiency packaging, (2) compatible with existing controlled deployment scheme, (3) requiring no or very low space power or curing agent, (4) producing no or very low in-orbit outgassing or contamination, (5) having predictable post-rigidization configuration accuracy, and (6) being adaptive to standard ground handling procedure and schedule (e.g., if a curing agent is needed, it must have a long enough shelf life in ambience to accommodate flight system integration, launch preparation and possible launch delays), (7) having a reversible rigidization process such that the rigidization process and post-rigidization configuration of the flight unit can be checked out and then re-packaged for launch. At this time, many space rigidization methods are being studied and developed. These include stretched aluminum laminate, hydro-gel rigidization, open-cell foam, and various polyester resins that are curable by space cold, heat, UV or IR. Of all known space rigidization methods, only the one that uses stretched aluminum laminate is judged to possess all of the above-listed desired features. Additionally, the space rigidization method of using stretched aluminum laminates also has two more important advantages: (1) it draws the rigidization pressure from the inflation system that is already needed for deployment and (2) both of the two component materials, the aluminum and Kapton of a typical aluminum laminate have long heritage of space applications. However, the stretched aluminum laminate rigidization method has two major shortcomings – low load-carrying capability and local failure modes. Since, due mainly to packaging constraints, only a very thin (no more than 0.004”) soft aluminum layer can be incorporated in the laminate, the inflatable/rigidizable booms made of stretched aluminum laminates buckle under very low axial loading due to local crippling. Local crippling is a failure mode induced primarily by surface and/or embedded imperfections in the boom walls that can vary from one boom to another, even they are of the same design. Before the stretched aluminum laminate method can become the preferred space rigidization method for inflatable structures, the load-carrying capability must be improved and the local failure mode eliminated.

SPRING-TAPE-REINFORCED ALUMINUM LAMINATE BOOMS

During the past three years, JPL has been continuously engaged in performing research efforts related to space inflatable structures, including long space-rigidizable booms made of stretched aluminum

laminates. It was during such an effort that the concept of a new kind of self-rigidizable space inflatable structures, identified as the spring-tape-reinforced (STR) aluminum laminate booms, or simply STR booms, was invented¹.

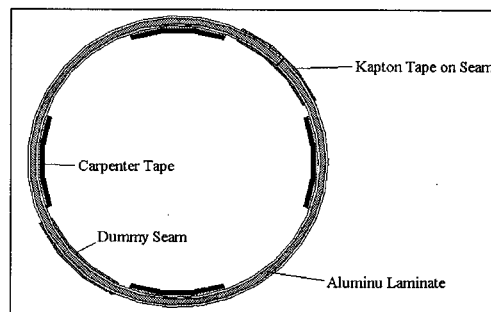


Figure 1. Cross-section of a typical STR aluminum laminate boom

A typical STR boom consists of a tube that is formed with aluminum laminate sheet and seamed by the Kapton tape and two endcaps. Figure 1 shows the cross-section of the aluminum laminate tube. In order to keep the boom straight after the inflation deployment, a dummy seam is placed on the opposite location (180 degrees apart) of the real seam. Four spring tapes are attached to the inside wall of the tube in axial direction. At this time, the commercially available stainless steel measuring tapes, commonly known as carpenter tapes, are used. With a wall thickness less than 4-mils, a STR boom can be easily flattened, rolled-up (or fold-up), and deployed by a relatively low inflation pressure. The buckling capability of a STR aluminum laminate boom is significantly improved mainly due to the high modulus of elasticity and curved cross-sectional profile of the spring tapes. The length of a STR boom can consequently be significantly increased. It should be pointed out that spring tapes are very effective in resisting inward buckling and the aluminum laminate wall is very stable in resisting outward buckling. Therefore, these two components effectively complement each other in resisting local crippling of the boom. In addition, unlike the non-reinforced aluminum laminate booms, a STR aluminum laminate boom relies on the reinforcing tapes, not pre-strain induced by high internal pressure, to attain its post-deployment stiffness. The required inflation pressure for a STR aluminum laminate boom is relatively low and that, in turn, reduces the load requirements for its seam.

BUCKLING TEST AND ANALYSIS

Axial buckling capability of the STR booms has been investigated in a previously reported research effort².

A brief summary is given here for the sake of completion.

Seven STR booms samples were designed, fabricated and buckling tested. These booms were 3 inches in diameter and 5 meters in length. The boom walls were made of an aluminum laminate that consists of a 3-mil-thick 1145-0 aluminum sheet with 1-mil-thick polyester films bonded on both sides. The reinforcement tapes were steel carpenters measuring tapes (commercial-grade tapes purchased from Sears). The nominal weight of each boom specimen (excluding the end caps) was slightly less than 0.9 Kg. Table 1 shows the results from buckling tests conducted on these sample booms with pin-pin end conditions.

Table 1. First-Time Buckling Test Results

Boom Sample #	Buckling Load (kgs.)	Buckling type
1	53.1	Euler
2	51.3	Euler
3	60.8	Euler
4	67.3	Euler
5	60.5	Euler
6	61.4	Euler
7	74.3	Euler

Since the seven sample booms were numbered in accordance with the order in which they were fabricated, the differences in the buckling loads were mainly due to improvements in boom fabrication and assembly, including better straightness and adhesive tapes. As the fabrication/assembly of booms improved from specimen #1 to specimen #7, the corresponding Euler's buckling load of the boom was asymptotically approaching the theoretical value of 75.2 Kgs (167 lbs) as predicted by analysis. Figure 2

shows the finite element model and the buckling analysis result of the STR aluminum laminate boom. This model is composed of 4802 nodes. 2364 plate elements were used to simulate aluminum laminate sheet. 2364 laminate elements were used to simulate the carpenter tape with aluminum sheet. 96 elements were used to simulate end caps. From figure 2 one can observe that the failure mode is Euler buckle.

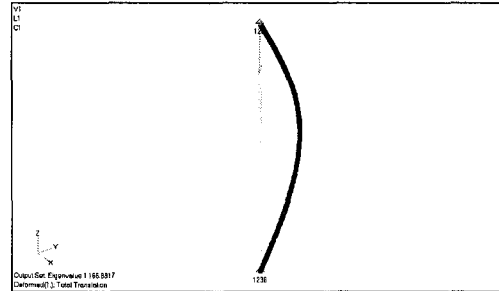


Figure 2. Finite-element model and buckling analysis of STR aluminum laminate boom

The buckling load predicted by the finite-element analysis is 75.2 Kgs (167 lbs). Compared to the best "first-time" buckling test result of 74.3 Kgs (165.2 lbs). The percentage difference between the analytical prediction and test result is:

$$\xi = 1 - \frac{\text{Test Result}}{\text{Analysis Result}} = 1 - \frac{165.2}{167} = 1\%$$

STOWED AND RE-DEPLOYMENT TESTS

In order to study the packaging efficiency and stowage effect of STR booms, a series of stowage and re-deployment test were performed on Booms #3 and #4. For stowage, the booms were flattened and

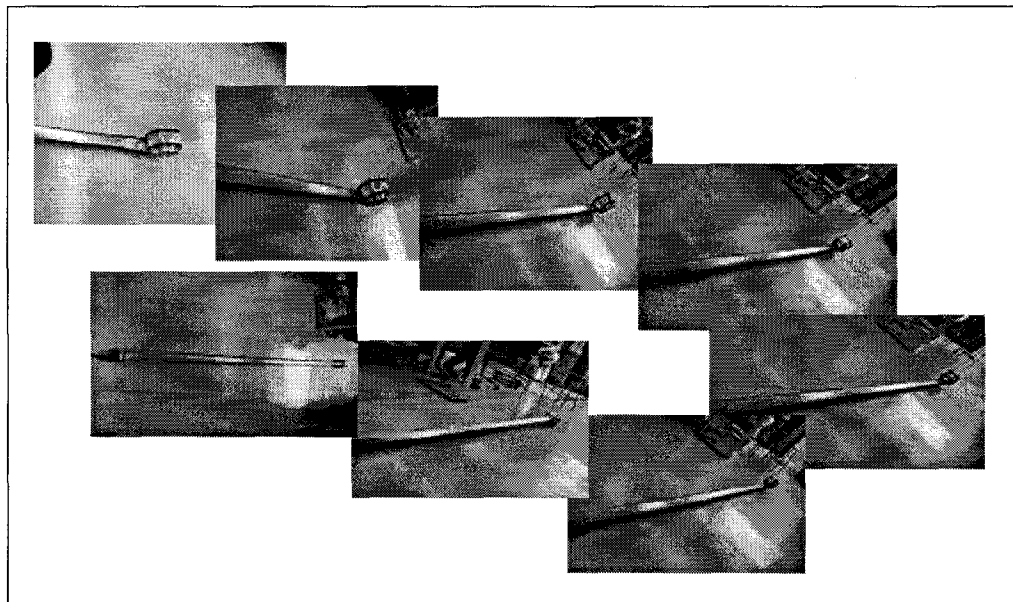


Figure 3. Inflation deployment of a 5-meter STR boom

rolled-up on a mandrel with a diameter of 6.5 inches or 12 inches before inflation deployment. Figure 3 shows the process of a typical inflation deployment. The deployment control technique using Velcro strips was employed.

A. Test Description:

- 1) Before being tested for the first time, both of Booms #3 and #4 were inflated for 5 minutes at 5 psi before testing. The buckling loads are 60.8 Kgs (135.2 lbs) for Boom #3 and 67.3 Kgs (149.6 lbs) for Boom #4.
- 2) After the buckling tests, both booms were flattened and tightly rolled up on mandrels. A 6.5" diameter mandrel was used for Boom #3 and a 12" diameter mandrel was used for Boom #4.
- 3) After 5 days in storage, Boom #3 was first unrolled. After the boom was unrolled, we found wrinkles along the edge in some areas. Figure 4 shows a close-up look of these wrinkles. These wrinkles may have been caused by the fact that the boom was not perfectly straight to begin with and the problem further compounded by the imperfect process of rolling up.



Figure 4. Wrinkles on Boom #3

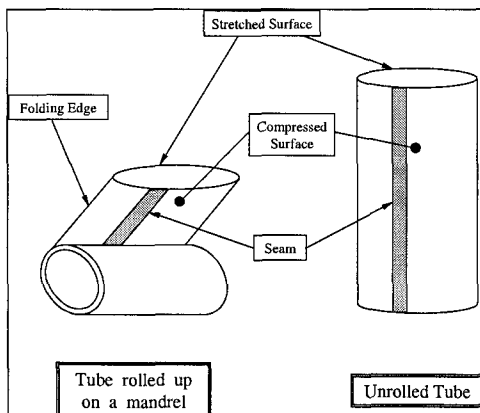


Figure 5. Terminologies

There are two terminologies need to be defined here. When we rolling-up the boom, one side of the boom faces the mandrel and is compressed. Let us call this surface as compressed surface and another surface as stretched surface.

After the boom was inflated at 5 psi for 5 minutes, these edge wrinkles almost disappeared. At this time, we saw some bigger wrinkles on the stretched surface. Figure 6 shows these wrinkles. One explanation of these wrinkles is that the stretched surface was elongated during the roll-up. Inflation wants to straighten the boom and induced these wrinkles. These wrinkles could be one of the causes of the buckling load decay.

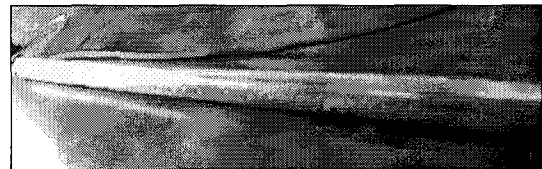


Figure 6. Wrinkles on Boom #3—After inflation

After inflation, Boom #3 was tested twice. The first test result was 41.4 Kgs (92.0 lbs) and the second test result was 40.1 Kgs (89.2 lbs). The boom was inflated at 5 psi for 5 minutes between two tests.

After the two tests, we kept the boom inflated at 5 psi for 2.25 hours. We noticed that 30% to 40% of wrinkles were removed. We repeated the buckling test again and the result was 42.3 Kgs (94.0 lbs). Keeping the boom pressurized for some time apparently helped to remove wrinkles and to straighten the boom. As a result, the buckling load increased.

Boom #4 was also unrolled and tested on the same day. Figure 7 shows boom #4 after been inflated. One can also see bigger wrinkles on the stretched surface of the boom. But they were not as severe as on boom #3



Figure 7. Boom #4—After inflation

Two buckling tests were conducted. The buckling loads of 47.5 Kgs (105.6 lbs) and 45.7 Kgs (101.6 lbs) were recorded respectively.

B. Test Results and Discussions

The post-stowage buckling test results are summarized in Table 2. In the Table, first time load refers to the first time buckling load recorded prior to rolling up of booms. Inflation time refers to the time that the booms were left pressurized.

Table 2. Buckling Test Results of Re-Deployed Booms

Boom #	Test #	Buckling loads (lbs)	Inflation Time
3	1	135.2 (First Time)	5 minutes
3	2	92.0 (Rolled up)	5 minutes
3	3	89.2 (Rolled up)	5 minutes
3	4	94.0 (Rolled up)	135 minutes
4	5	149.6 (First Time)	5 minutes
4	6	105.6 (Rolled up)	5 minutes
4	7	101.6 (Rolled up)	5 minutes

We observe that the buckling load decreased each time we repeated the test on the same boom except for test #4 on Boom #3 when it was kept pressurized for an extended period of time.

Comparing tests #2 and #3 for Boom #3, buckling load was reduced by 2.8 lbs. Assuming the same would have happened if the boom were never rolled, the percent reduction of the load on Boom #3 due to rolled up (on a 6.5" mandrel) is:

$$(135.2-92.0-2.8)/(135.2-2.8)=31\%$$

Applying the same reasoning for Boom #4, we find the percent reduction of the load on Boom #4 due to rolled up (on a 12" mandrel) is:

$$(149.6-105.6-4.0)/(149.6-4.0)=27\%$$

Comparing test #3 and #4, we find the percent increase of the load due to continuous pressurization of the boom is:

$$(94.0-89.2+2.8)/(89.2-2.8)=9\%$$

From these test data, we can have following observations:

After a boom is rolled up for stowage and later unrolled, its strength to resist buckling is reduced. During the roll-up, the aluminum skin on the outside of the boom is stretched while the skin on the inside of the boom is compressed. After the boom is unrolled and inflated, the uniform internal pressure

causes the outside surface of the boom to wrinkle. This may be the primary reason for the decrease in buckling resistance.

- ◆ The wrinkles along the edges of the flattened boom are easier to be removed by inflation pressure than the wrinkles on the surfaces.
- ◆ The diameter of the mandrel appears, at least in the range of 6.5 to 12 inches, not to significantly affect the buckling load of the re-deployed boom.
- ◆ Keep the re-deployed boom under inflation pressure booms has noticeably improved its buckling capability.

DYNAMIC TEST AND ANALYSIS

Dynamic characteristics of a 5-meter STR boom have been analyzed and test-verified. The boom also has a 3-mil aluminum laminate wall and is 3 inches in diameter. The boundary condition of the boom is fixed (top)—free (bottom).

A. Dynamic Test Results

Figure 8 gives a typical frequency response spectrum obtained from dynamic testing on the STR boom. The input excitation and output response are both measured and recorded at the lower (free) end of the boom.

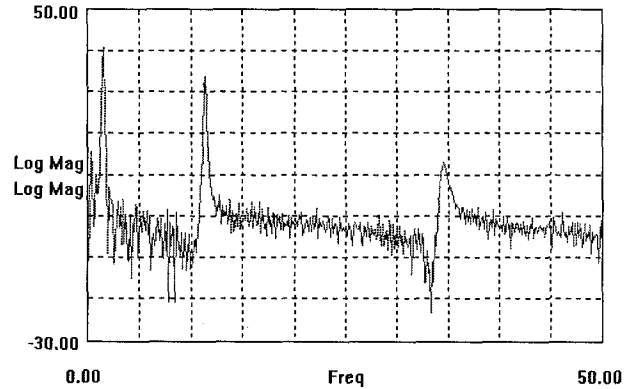


Figure 8. A typical frequency response spectrum

The first three resonant frequencies are obtained as 1.46 Hz, 11.30 Hz, and 34.31 Hz.

B. Dynamic Analysis

A high-fidelity finite element model has also been assembled for the boom sample used in the dynamic testing. This model is composed of 4802 nodes. 2364 laminate elements are used to model the aluminum laminate areas. 2364 laminate elements

are used to model the carpenter tape areas. 96 elements are used to represent the end caps. Figure 9 shows the finite-element model used for dynamic analysis of the STR boom.

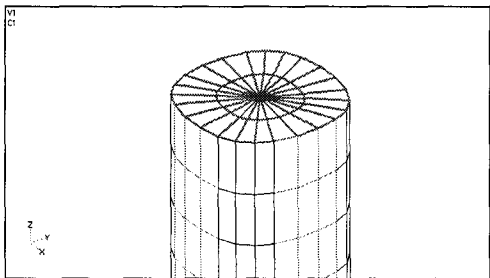


Figure 9. The dynamic analysis finite element model

The finite-element analysis predicted the first three global frequencies at 1.47 Hz, 11.54 Hz, and 34.21 Hz. Table 3 compares the analytical predictions with the results of actual dynamics testing. The maximum difference is only 1.3% for the 2nd mode frequency.

Table 3. First three global frequencies obtained from test and analysis

	1 st global frequency	2 nd global frequency	3 rd global frequency
Test	1.46 Hz	11.30 Hz	34.31 Hz
Analysis	1.47 Hz	11.54 Hz	34.21 Hz
Differences	0.7%	1.3%	0.3%

Figures 10 through 12 show the mode shapes of these three global modes.

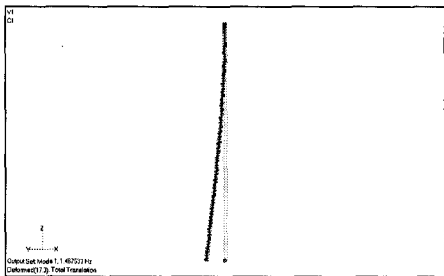


Figure 10. The first global mode shape

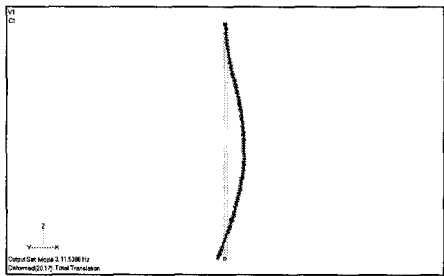


Figure 11. The second global mode shape

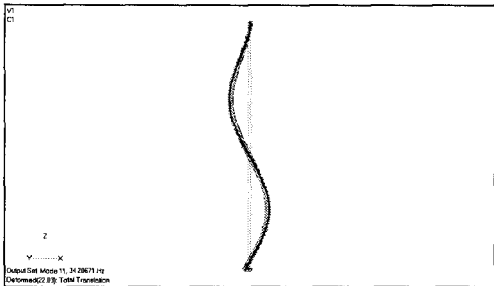


Figure 12. The third global mode shape

This finite element model calculated 11 modes between 0 to 34.5 Hz. Because of symmetry, the 1st mode is identical to the 2nd mode, which is the first global mode. The 3rd mode is identical to the 4th mode, which is the second global mode. The 11th mode is identical to the 12th mode, which is the third global mode. There are 6 local modes between the second global mode and the third global mode. Mode shapes of these local modes are represented by figure 13 to figure 18.

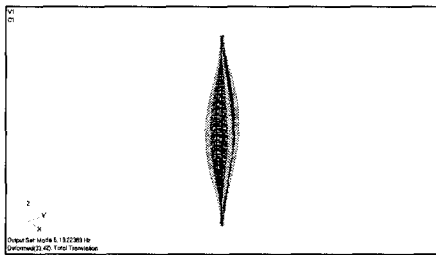


Figure 13. The 5th mode

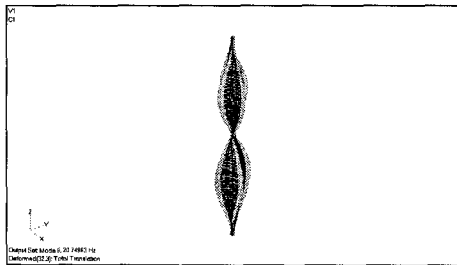


Figure 14. The 6th mode

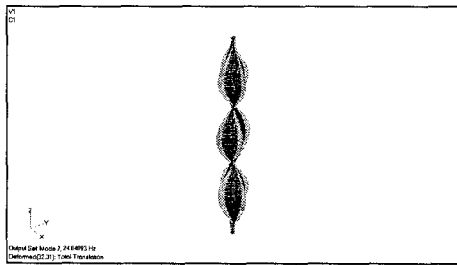


Figure 15. The 7th mode

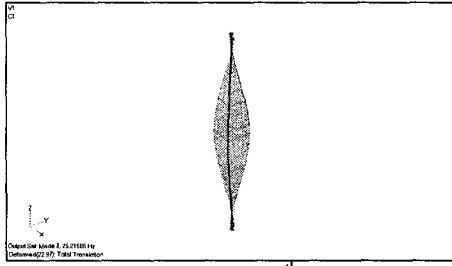


Figure 16. The 8th mode

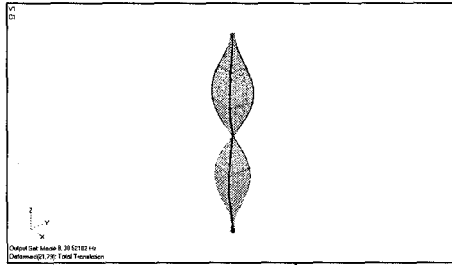


Figure 17. The 9th mode

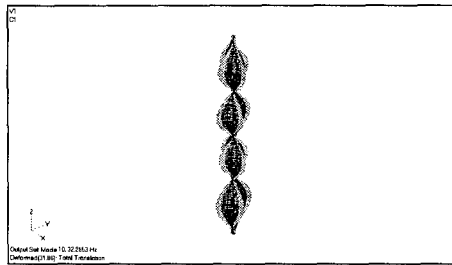


Figure 18. The 10th mode

BEAM SIMULATION OF A STR BOOM

In an attempt to reduce modeling and computational efforts, the feasibility of modeling a STR boom by a simple beam, instead of laminate and solid elements, was investigated. This effort was based on the following basic data of a sample STR boom: The weight of the boom is 0.9 Kg (2 lbs). The weight of the end cap is 0.366 Kg (0.8125 lbs). The length of the boom is 5 meters (197 inches). The first frequency, as predicted by finite element analysis is 1.4675 Hz.

The fundamental frequency of a slender beam with concentrated mass at one end and another end is fixed can be calculated by equation³:

$$f_1 = \frac{1}{2} \left[\frac{3EI}{L^3 (M_{\text{beam}} + 0.24M_{\text{mass}})} \right]^{\frac{1}{2}}$$

Based on the given data, the value of EI (i.e., the product of Young's modulus and moment of inertia) of the beam is calculated to be 718,102 lb-in².

A new finite element model was created. This model is composed of a single beam element with a length of 197 inches and an EI of 718,102 lb-in². At the bottom of the beam, there is a 0.8125 lbs lumped mass that is used to represent the endcap. The top of the beam is fixed and the bottom of the beam is free. The first three natural frequencies and mode shapes are calculated. Table 4 gives first three global frequencies calculated by using laminate elements and beam elements.

Table 4. Frequencies of laminate element model and beam element model

Element type	1 st global frequency	2 nd global frequency	3 rd global frequency
Laminate	1.47 Hz	11.54 Hz	34.21 Hz
Beam	1.46 Hz	11.62 Hz	35.26 Hz
Differences	0.7 %	0.7 %	3.1 %

The first and second natural frequencies of these two models are very close. The third natural frequencies of these two models are different by more than 3%. One reason is that, during the first and second modes, the cross-section of the laminate element model doesn't have noticeable change, (see Figures 19 and 20). However, for the 3rd mode, one can see from figure 21 that the cross-section of the boom has obviously changed from a circular shape. Therefore, beam element model should not be used to calculate high frequency characteristics.

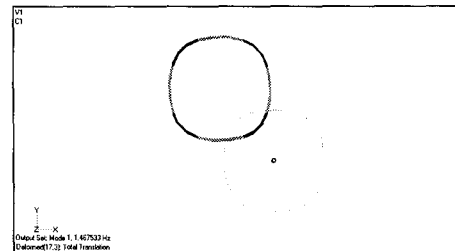


Figure 19. Deformed cross-section of the 1st mode

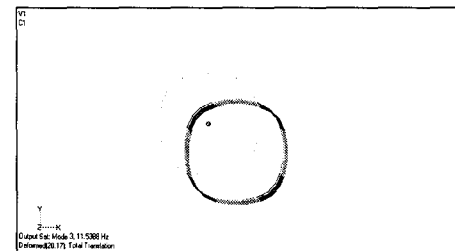


Figure 20. Deformed cross-section of the 2nd mode

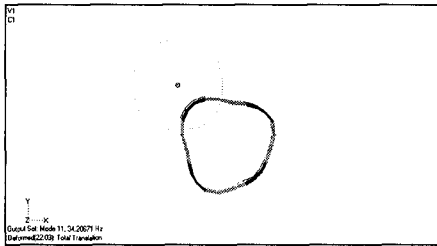


Figure 21. Deformed cross-section of the 3rd mode

EXTENSION OF BOOMLENGTH AND CAPABILITY

An assessment of the load-carrying requirements of potential space applications of the STR booms, the maximum boom length is estimated to be about 10 meters. This estimate is based on that the boom is made of commercially available carpenter tapes, which put an arbitrary limit on the boom diameter to be 3 inches.

To extend this maximum useful boom length, we are considering the concept of clustered booms. A clustered boom is formed by structurally joining three, four or more individual STR booms together. A preliminary analytical study has been conducted and shown that a clustered boom yields significantly high buckling strength than a single STR boom. It is believed that the clustered booms can reach a length of over 50 meters. Inflation deployment of clustered booms is also inherently stable and the need for adding deployment control devices may be eliminated.

However, there remain many practical issues for the design and fabrication of clustered booms that need to be resolved. These include the joining of booms, packaging schemes, and deployment mechanisms.

Other design improvements for enhancing structural integrity and the load-carrying capability of STR booms that are currently being considered are: (1) addition of circumferential reinforcements, (2) improved laminates materials, (3) larger boom diameters, and (4) longitudinal reinforcing tapes made of fiberglass/epoxy composite, graphite/epoxy composite, titanium, or other high-toughness materials. In addition, a new generation of modeling and analysis tools is also being developed specifically for space inflatable and rigidizable structures, including the STR booms. For example, see⁴.

CONCLUDING REMARKS

The STR booms represent a new and innovative type of space inflatable and rigidizable structures. Through the development process, including design, analysis, fabrication, assembly, and testing, many

distinct advantages of the STR booms have been identified and demonstrated. These include:

- Simplicity of the design
- Self-rigidizable in space
- High load-carrying capability
- High packaging efficiency.
- Failed by Euler's buckling (which is easy to predict) instead of local crippling
- Required low inflation deployment pressure
- Using space qualified materials with negligible outgassing and contamination
- Reversible for repeated ground testing

Additional research efforts on the STR booms will be performed to study the clustered booms and other design features that will improve the load-carrying capability of STR booms. Work has also been initiated to study design methodologies and potential applications of two- and three-dimensional space inflatable structures that use the STR booms as the building-block elements.

ACKNOWLEDGEMENTS

The authors wish to thank Pierre Leung, Grigor Kerdanyan, and Joel Rodriguez all of California State University at Los Angeles, for their contributions to this research effort. The work described was performed at Jet Propulsion Laboratory, California Institute of Technology under contract with the National Aeronautics and Space Administration.

REFERENCES

- [1] Fang, H. and Lou, M., "Tape-Spring Reinforcements for Inflatable Structural Tubes," NPO-20615, NASA Tech Briefs, Vol 24, No. 7, July 2000.
- [2] Lou, M., Fang, H., and Hsia, L., "A Combined Analytical and Experimental Study on Space Inflatable Booms," presented at the 2000 IEEE Aerospace Conference. Big Sky, Montana, March 2000.
- [3] Robert D. Blevins, "Formulas for natural frequency and mode shape," Krieger Publishing Company, 1979.
- [4] Yang, B., Lou, M., Ding, H., and Fang, H., "Buckling Analysis of Carpenter-Tape-Spring Reinforced Inflatable Struts," presented at the 41st AIAA Structures, Structural Dynamics and Materials Conference, Atlanta, GA, April 2000.